Title

Frequency-specific network connectivity increases underlie accurate spatiotemporal memory retrieval

Journal

Nature Neuroscience, 16(3)

ISSN

1097-6256

Authors

Watrous, Andrew J
Tandon, Nitin
Conner, Chris R
et al.

Publication Date

2013-03-01

DOI

10.1038/nn.3315

Peer reviewed

HHS Public Access

Author manuscript

Nat Neurosci. Author manuscript; available in PMC 2013 September 01.

Published in final edited form as:

Nat Neurosci. 2013 March ; 16(3): 349–356. doi:10.1038/nn.3315.

Frequency–specific network connectivity increases underlie accurate spatiotemporal memory retrieval

Andrew J. Watrous[1,2], **Nitin Tandon**[3,4], **Chris Connor**[3,4], **Thomas Pieters**[3,4], and **Arne D. Ekstrom**[1,2,5]

[1]Neuroscience Graduate Group, University of California, Davis

[2]Center for Neuroscience, University of California, Davis, 1544 Newton Court, Davis, CA

[3]Department of Neurosurgery, University of Texas Medical School, Houston, Texas

[4]Memorial Hermann Hospital – Texas Medical Center, Houston, Texas

[5]Department of Psychology, University of California, Davis, CA

Abstract

The medial temporal lobes, prefrontal cortex, and parts of parietal cortex form the neural underpinnings of episodic memory, which includes remembering both where and when an event occurred. Yet how these three key regions interact during retrieval of spatial and temporal context remains largely untested. Here, we employed simultaneous electrocorticographical recordings across multiple lobular regions, employing phase synchronization as a measure of network functional connectivity, while patients retrieved spatial and temporal context associated with an episode. Successful memory retrieval was characterized by greater global connectivity compared to incorrect retrieval, with the MTL acting as a convergence hub for these interactions. Spatial vs. temporal context retrieval resulted in prominent differences in both the spectral and temporal patterns of network interactions. These results emphasize dynamic network interactions as central to episodic memory retrieval, providing novel insight into how multiple contexts underlying a single event can be recreated within the same network.

Keywords

human memory; ECoG; network analysis; oscillations; phase synchronization; delta; theta

Introduction

Successfully recalling an event in our everyday life depends critically on retrieving the context associated with it. A memory, such as what we ate for dinner last night, is more

CORRESPONDING AUTHOR: Dr. Arne Ekstrom, PhD, Center For Neuroscience, University of California, Davis, 1544 Newton Court, Davis, CA 95618, Phone: 530.757.8850, adekstrom@ucdavis.edu.

Author Contributions:

A.D.E., N.T., and A.J.W. designed the experiment. N.T., C.C., and T.P. collected the data. A.J.W. performed the data analysis. A.J.W., A.D.E., and N.T. wrote the manuscript.

vividly recreated when we can remember contextual details, such as the location of the restaurant[1]. Neuroimaging and patient lesion studies strongly support the contributions of specific brain regions to episodic memory retrieval, emphasizing selective roles for the medial temporal lobe (MTL)[1–7], prefrontal cortex[2, 3, 6, 8, 9], and parts of parietal cortex[2, 10–12] in this process. Distributed, coordinated activity across brain regions is also critical to memory retrieval[13–18], with synchronized activity in the local field potential (LFP) implicated in coordinating this process[19]. Specifically, low–frequency (3–12 Hz) coordinated activity between hippocampus and prefrontal cortex in rodents is related to learning new rules during a spatial navigation task[20] and can bias neocortical neuronal firing[21, 22]. The theoretical perspectives emerging from such work appear to provide conflicting accounts of whether successful memory retrieval is primarily mediated by a specific brain region (Figure 1A, upper), is best characterized by changes in functional connectivity between multiple brain regions (Figure 1A, lower), or is some combination of the two.

Recalling a prior experience often involves retrieving multiple, disparate[2] types of context, e.g., not only where we ate dinner, but when it occurred relative to other events. Assuming that specific contextual information is represented by distinct cell assemblies within the same or overlapping brain regions[13–16], how do different context representations emerge from within constituents of the same network? Although regional specificity may provide one possible account of this issue[23, 24], another interesting proposal, the so–called spectral–fingerprint hypothesis, argues that different cognitive operations manifest as distinct, *frequency–specific* patterns of interregional phase synchronization in large–scale networks[25, 26]. These frequency–specific phase interactions are a strong candidate mechanism for coordinating distributed cell assemblies in parallel[27–29], known as “frequency multiplexing,” and may underlie the rapid retrieval of contextual information specific to a particular experience (Figure 1B). While previous studies suggest the importance of low–frequency band power modulations in the MTL using resting MEG (between 4–6Hz)[30] and coherence during human free recall tasks using intracranial EEG (at ~3 and 8Hz)[31,32], how and in what manner frequency multiplexing occurs between brain regions involved in retrieval of episodic memory is not known.

We set out to test two fundamental sets of theoretical perspectives on the neural basis of episodic memory retrieval. The first regards whether accurate episodic memory retrieval is characterized by a disproportionate contribution of a specific brain region and/or accomplished by changes in global connectivity across the network (Figure 1A). The second addresses how different contexts can be retrieved via interactions within the same set of brain regions (Figure 1B). Specifically, to address the second issue, we test the above two possibilities regarding regional vs. global changes in connectivity along with the spectral fingerprint hypothesis. To directly test these ideas, we employed electrocorticographical (ECoG) recordings in patients undergoing clinical monitoring, focusing on three areas strongly implicated in past literature as central to episodic memory: parahippocampal gyrus ([PHG], that serves as a “gateway” to the hippocampus[5, 33], see Methods), parietal cortex, and lateral prefrontal cortex (Supplementary Figure 1). We did this by comparing low–frequency (1–10 Hz) phase synchronization between these key regions, which we term “the

retrieval network," as patients performed a task requiring both spatial layout and temporal order memory retrieval (see Methods and Figure 1C–E). By measuring whether retrieval manifested as changes in connectivity between specific regional "hubs," changes in global connectivity, or was best characterized by specific changes in spectrotemporal dynamics, our approach allowed us to directly test these different theoretical models regarding the neural basis of episodic memory.

Results

Evaluation of simultaneously recorded ECoG signals revealed prominent low frequency phase consistency between PHG and specific sub–regions of parietal and prefrontal cortex (Figure 2A,2B; Supplementary Figure 2 & 3) when patients accurately retrieved spatiotemporal contextual information. On individual electrode pairs, correct context retrieval was accompanied by increases in PHG–parietal and PHG–prefrontal pairwise phase consistency beginning at the onset of retrieval (Figure 2C,D, and Supplementary Figure 4; see Online Methods for Pairwise Phase Consistency [PPC] description). Similar findings were also evident at the population level: we found significantly ($p_{fwe} < .05$) increased low frequency PPC during correct retrieval across the network, for instance, between PHG–parietal (PHG–IPL [Figure 2E]) and PHG–prefrontal (PHG–MFG [Figure 2F]) recordings (Supplementary Figure 5; see Methods for statistical approach). Control analyses examining individual electrode raw traces (Supplementary Figures 2 & 3) and regional power modulations (Supplementary Figure 6) revealed that oscillatory power typically increased following cue onset. This regional increase in oscillatory power, however, was not condition specific (Supplementary Figure 6), suggesting that our PPC changes could not be accounted for by regional power changes alone (i.e., compare Supplementary Figures 5 vs. 6).

Network Connectivity during Correct & Incorrect Retrieval

To evaluate coherent phase interactions globally across the brain, we adopted a graph theoretic approach[34]. We treated each subregion (e.g., MFG, IPL, PHG) as a node in a network functionally connected via phase synchronization at a given time and frequency (Figure 3A–E; see caption and Online Methods for description of network construction). We found the greatest PHG connectivity in the low frequency (1–10Hz) band compared to other bands (Figure 4A and Supplementary Figure 7; $\chi^2(3) = 70.48, p < .0001$), consistent with previous findings that have suggested MTL networks operate preferentially within the delta–theta band[31, 35, 36]. We therefore restricted subsequent analyses to the low–frequency band. Figure 4B shows the networks associated with correct and incorrect memory retrieval at 3,5, and 8 Hz. We found significantly more interregional pairs (henceforth referred to as network "edges") that showed significant task–related low frequency PPC increases during correct retrieval than during incorrect retrieval at every frequency up to 9 Hz (Figure 4C lower panel, blue asterisks; all $\chi^2(1) > 12.93$, all $p < .0008$). This finding held true when we compared the distribution of connectivity between conditions at each frequency band across subregions, (each $\chi^2(6) > 98$, $p < .0001$) and for each subregion across 1–9 Hz frequency bands ($\chi^2(8) > 100$, $p < .0001$). It was also robust to comparisons between nearly all subregions and frequencies individually (Figure 4B,C; compare Figure 4C top panel to Figure 4C middle panel, binomial tests, $p < .05$). Thus, rather than discrete switches in

regional specificity within the network during correct vs. incorrect retrieval, or changes in preferred frequency, our findings suggest instead that network connectivity increases globally during correct vs. incorrect retrieval processes across these low frequencies (Figure 4B, compare top panel [correct] vs. bottom panel [incorrect] and Figure 4C, lower panel, compare red vs. blue bars).

Despite overall increases in connectivity across the "retrieval network" during correct memory retrieval, it could be the case that specific subregions still acted as "hubs," that is, some subregions showed greater levels of connectivity compared to other subregions. To address this, we measured node degree, the total number of connections a node has with all other nodes. Following previous work[34], we determined whether there were hubs in the network based on the distribution of node degree being different than a uniform network; a hub was then defined to be the node showing the highest degree of connectivity. We found that node degree varied significantly compared to a uniformly distributed network and that PHG had the greatest number of connections compared to other nodes across several low frequency bands (Figure 4B,C upper panels, red asterisks: 1Hz $\chi^2(6)=15.4$, $p < .02$; 4Hz, 7–9Hz $\chi^2(6)>18$, $p < .005$ for all comparisons). This analysis demonstrates that PHG acts as a "hub" for interactions during accurate episodic memory retrieval. Notably, PHG node connectivity did not vary across frequencies ($\chi^2(9)=6.9$, $p=.64$), indicating that it acts as a hub for information transfer across all low frequency bands. Because the PHG serves as a gateway to the hippocampus[33,5], these findings are consistent with many decades of work that point to the importance of the medial temporal lobes in coordinating episodic memory retrieval[1–7].

Network Connectivity during Spatial & Temporal Retrieval

Our behavioral paradigm involved retrieving both the location of an item within the spatial layout and its temporal order relative to other items (see Methods). We were therefore able to evaluate differences across identical patients, recording zones, and visually identical experimental paradigms (differing only on remembering spatial vs. temporal information) during retrieval of spatial or temporal contexts (Figure 1C–E). We then evaluated whether this led to changes in interregional connectivity, global connectivity, or frequency–specific differences in connectivity (Figure 1A–B). Our findings primarily support the third possibility. Phase coherent oscillations in the raw trace were visually evident in a lower frequency band during spatial retrieval trials (Figure 5A, upper) compared to temporal retrieval (Figure 5A, lower); this difference was also evident in comparisons at the patient (Figure 5B) and at the population level (Figure 5C; statistical methods identical to those in Figure 2E & 2F).

Using our graph–theoretic approach, we also found that these behavior–specific and frequency–dependent phase interactions were present across the network. Comparing node connectivity overall within the network, we observed significantly greater connectivity between nodes during spatial retrieval compared to temporal retrieval from 1–4 Hz (Figure 5D, all $\chi^2(1) >14.61$, all $p < .0002$; also see Figure 5G–J). In contrast, we observed significantly greater connectivity between nodes during temporal compared to spatial retrieval from 7–10 Hz (7–8Hz $\chi^2(1) >16.5$, $p < .0001$; 9–10Hz $\chi^2(1) >4.1$, $p < .05$). For

spatial retrieval, 6 of 7 of nodes showed greater functional connectivity in the 1–4 Hz band compared to the 7–10 Hz band (Figure 5E; Chi–square test between bands; all$\chi^2(1) > 9.13$, all $p < .003$). In contrast, during temporal retrieval, 6 of 7 nodes showed differential connectivity in the 7–10 Hz band (Figure 5F; all $\chi^2(1) > 11.3$, all $p < .001$). We confirmed a lower preferred frequency during spatial retrieval both across subjects (Figure 5K, $t(5) = 2.44$, one–tailed $p = .029$) and across electrode pairs ($t(664) = 4.43$, $p < .000001$). These findings demonstrate that the "retrieval network" resonates at a lower frequency overall during spatial compared to temporal retrieval.

Despite these differences in the preferred frequency in which connectivity manifested, the PHG node again showed the highest degree of connectivity compared to any other node during both spatial and temporal retrieval (Figure 5E,F). During spatial retrieval, PHG showed the greatest connectivity in the 1–4 Hz band (Figure 5G) while during temporal retrieval, PHG showed the greatest connectivity in the 7–10 Hz band (Figure 5J). During spatial retrieval, we found that the PHG node connections were primarily clustered with SFG, MFG, and PCN (Figure 5G $\chi^2(5)= 32.63$, $p < .00001$) and there was significantly more PHG connectivity with these nodes in the 1–4 Hz band compared to the 7–10Hz band ($\chi^2(5)= 208.65$, $p < .00001$). In contrast, during temporal order retrieval, PHG connections were preferentially clustered with SFG, MFG, and IPL (Figure 5J; $\chi^2(5)= 19.09$, $p < .002$) and there was significantly more PHG connectivity with these nodes in the 7–10 Hz band compared to the 1–4Hz band ($\chi^2(5)= 78.58$, $p < .00001$). These differences amounted to a significant condition (spatial vs. temporal) by frequency (1–4 Hz vs. 7–10 Hz) interaction in PHG connectivity (Fisher's Exact test, $p < .00001$). Follow–up analyses separately assessing the spatial correct vs. spatial incorrect and temporal correct vs. temporal incorrect networks showed similar results to those directly contrasting spatial correct vs. temporal correct (Supplementary Figure 8). These findings show that retrieving spatial layout vs. temporal order information from an episode was characterized *primarily* by frequency–specific interactions across the retrieval network. Just as in our earlier analyses, however, PHG had the highest degree of connectivity within the network compared to any other node, suggesting its central importance to both spatial and temporal retrieval.

We also evaluated whether spatial and temporal retrieval were characterized by changes in timing of connectivity within their preferred frequencies. For all pairwise combinations of regions within the network, we calculated the connectivity map for the two different conditions based on a matrix of spatial vs. temporal PPC difference scores at 2Hz (Figure 6A) and 8Hz (Figure 6B). During spatial retrieval, significantly more connectivity occurred early (0–1 second) while during temporal retrieval, significantly more connectivity occurred late (1–2 seconds) (Figure 6C–D; Fisher's exact test, $p<.0001$). Visual inspection of the matrix of network connectivity suggested that spatial and temporal retrieval were also characterized by different clustering of connectivity across regional pairs (Figure 6A,B; Supplementary Movies S1 and S2). We confirmed this impression by computing the Phi correlation coefficient of binary connections over time (see Methods), with higher correlation coefficients indicating a more coherent pattern of activity across the entire network and lower correlation coefficients indicating a less coherent pattern of activity across the network. The distribution of correlation coefficients differed between spatial and

temporal retrieval (Figure 6E, Kolmogorov–Smirnov test, p<.0001) and the connectivity in the 2Hz spatial network was significantly more clustered in time than the 8Hz temporal network (Figure 6F, t–test (189)= 5.77, p < .0001). Critically, though, 1) these two networks did not differ in their total number of connections (see Figure 5D,$\chi^2(1)= .81$, p=.37), 2) we found similar results at adjacent frequencies (Supplementary Figure 9A), 3) and the findings could not be accounted for by the expected increase in temporal autocorrelation at lower frequencies (Supplementary Figure 9B). These results confirm that the connectivity during spatial and temporal retrieval, in addition to being characterized by different resonant frequencies, also displayed differences in the pattern of connectivity over time.

Finally, our results could not be accounted for by poor patient performance nor a difference in performance between spatial and temporal retrieval. Patients performed significantly above chance ($t(5) = 3.58$, $p = .015$) and showed similar reaction times in both the spatial and temporal tasks. Neither accuracy ($t(5) = -.56$, $p = .59$) nor reaction time ($t(5) = -1.00$, $p = .35$) differed between the spatial (71% accuracy; 7.57s median RT) and temporal (76% accuracy; 8.99s median RT) retrieval conditions. Our results were also robust at more stringent statistical thresholds (p<.001, Supplementary Figure 10).

Discussion

In this work we sought to determine the functional network interactions amongst brain regions previously implicated in successful episodic memory retrieval and to determine how multiple contextual representations characterizing an episode were retrieved within this network. We tested three fundamental theoretical models to determine whether one, or a combination of these, best characterized the neural basis of episodic memory retrieval. These included the following: 1) a model in which a single brain region acted as a hub for mediating episodic memory retrieval, 2) a model in which interactions were distributed relatively equally across nodes yet changed for successful retrieval or retrieval of different contexts, 3) a model in which changes in spectrotemporal dynamics mediated memory retrieval (see Figure 1). Our first set of analyses compared correct vs. incorrect context retrieval, collapsing across spatial and temporal retrieval trials. We found that successful memory retrieval was characterized by increases in network functional connectivity via phase synchronization across the 1–10 Hz low frequency band. PHG electrodes showed the highest degree of inter–connectivity with other electrodes compared to any other subregion within the “retrieval network” and this functional connectivity preferentially occurred in the 1–10Hz band. The macro–electrodes located over the PHG likely captured signals from posterior parahippocampal, perirhinal, and entorhinal cortices (see Methods), all of which provide direct input to the hippocampus[5, 33, 37], suggesting the likelihood that the hippocampus also participated in these interactions. Overall, while our findings of increased network connectivity during correct vs. incorrect context retrieval support the idea of global rather than regionally–specific changes in connectivity (Figure 1A, lower), the differentially enhanced PHG connectivity we observed supports the idea that the MTL acted as a hub in these interactions (Figure 1A, upper). Thus, our results support a hybrid of the two models put forth in Figure 1A, suggesting that successful memory retrieval is best characterized by an overall increase in interactions across key brain regions mediated primarily by the MTL. To our knowledge, this has not been demonstrated previously with invasive human

recordings that can pinpoint and disambiguate activity simultaneously across multiple brain regions.

Our results also emphasize the importance of phase–synchronized oscillations between these disparate brain regions as important to memory retrieval. Together with studies examining episodic encoding[38] and working memory[39, 40], our results, which were obtained during retrieval, suggest that phase coding may be a mechanism involved in an array of human memory processes. Previous proposals[19,25,41] suggest that synchronized oscillations may facilitate precisely–timed depolarizations between neurons in communicating brain regions. This idea is supported by the observation in humans [27,28], rats[20],and monkeys[29] that oscillations coordinate both local and distant neuronal activity. Furthermore, an influential theoretical model of memory retrieval, Multiple Trace Theory (MTT)[17], argues that cortical areas represent features bound to experience–specific contextual representation in the hippocampus, whose successful interaction underlies memory retrieval. Thus, our results provide evidence for a possible neural mechanism underlying MTT, namely, coordinated low frequency oscillations between the medial temporal lobe and cortical areas.

Taken together, our results yield a potentially new perspective on previous findings regarding the importance of MTL, parietal cortex, and prefrontal cortex in mediating successful episodic memory retrieval. Several fMRI studies show increased parietal cortex activation during episodic retrieval tasks [1–3, 10, 11] yet lesions to this area in human patients do not consistently impair episodic memory[10]. Similarly, prefrontal cortex activation is often a hallmark of successful memory retrieval yet prefrontal cortex lesions produce nuanced impairments in episodic memory retrieval[8]. For example, prefrontal cortex lesions impact free but not cued recall and are thought to affect executive processes but not retrieval of memory traces specifically[9]. In contrast, fMRI studies consistently show hippocampal and parahippocampal activation during correct recollection of specific contextual details[2, 3] and hippocampal lesions in particular profoundly impair recollection and episodic memory[7, 42]. Our results thus suggest that while lateral prefrontal and parietal areas communicate with the MTL during spatiotemporal retrieval, the MTL acts as a critical convergence “hub” during successful context retrieval, broadly consistent with MTT[17]. One possible interpretation of our results is that the MTL serves as the primary locus for indexing particular memory traces, with parietal and lateral prefrontal cortex interacting with the MTL to facilitate and augment memory trace retrieval[17, 18].

Epilepsy is a disease marked by impaired episodic memory performance and increased synchronized activity of large numbers of neurons which may manifest as low frequency phase synchronization. Do these factors confound our results? We believe several considerations weigh against this possibility. First, electrodes showing ictal and interictal discharge were systematically removed from our analysis based on evaluation by our clinical team. All analyzed trials were visually inspected for artifacts related to epilepsy. Next, disease related low frequency phase synchronization is likely to impair brain function and may interfere with accurate memory retrieval. Therefore, we would expect more low frequency phase coherence during incorrect compared to correct retrieval if ictal discharge alone accounted for our results, which is inconsistent with our findings. Third, it seems unlikely that epileptic activity would manifest itself as task–related (spatial vs. temporal)

differences. Finally, we utilized a metric of phase synchronization which excluded phase differences centered around 0 degrees (see Methods) to eliminate possible effects of volume conduction and any remaining epileptic synchronization. We note that this also excluded "true" zero–phase lag synchronization (increasing Type 2 error) but provides a more conservative estimate of interregional coupling. Although we observed increases in phase synchronization, this does not imply nor require direct anatomical connectivity between areas, and is instead taken primarily as a measure of functional connectivity. In summary, we have made every available effort to account for possible confounds while still capitalizing on the increased spatiotemporal resolution afforded by direct human brain recordings. Thus, we believe that our results, which provide novel insight into the dynamic networks underlying spatiotemporal episodic memory, would generalize to the population if these issues could be studied non–invasively.

Our behavioral paradigm also allowed us to compare retrieval of two different fundamental components of episodic memory, spatial and temporal context. Here, our results suggested that correct retrieval of the location of an item involved lower frequency interactions compared to correctly retrieving the order in which an item occurred relative to other items. While we again found that correct retrieval was characterized by higher degrees of connectivity compared to incorrect retrieval for the two processes separately (Supplementary Figure 8), the overall level of connectivity did not differ between spatial vs. temporal retrieval (Figure 5D). We also found differences in regional connectivity during spatial (PHG–SFG–MFG–Precuneus) vs. temporal (PHG–SFG–MFG–IPL) retrieval, with the critical difference being the subregions of parietal cortex engaged. Thus, our findings here primarily support the spectral fingerprint hypothesis[25] (Figure 1B), with some regional specificity within parietal cortex (Figure 1A, upper) but no clear differences in overall connectivity (Figure 1A, lower). Because in both cases PHG acted as a hub for interactions, our results suggest that spatial vs. temporal retrieval involved similar degrees of connectivity with the MTL. In a previous fMRI study using a similar behavioral paradigm, we found similar degrees of hippocampal activation during spatial and temporal retrieval along with greater activation in precuneus during a contrast of spatial vs. temporal retrieval[24] and, in another study, greater functional connectivity between hippocampus and precuneus during spatial retrieval [43]. Other studies have also implicated parts of inferior posterior parietal cortex in temporal processing[44]. Notably, however, many of the same regions in lateral prefrontal, MTL, and parietal cortex remained significantly connected in both networks. Thus, the most salient differences between the networks for retrieval of spatial vs. temporal context, in contrast to our findings with correct vs. incorrect retrieval, was the spectrotemporal dynamics at which the two networks operated, again consistent primarily with the spectral fingerprint hypothesis (Figure 1B).

Our results thus provide a new basis for resolving the question of how multiple contexts underlying an episode can be stored and retrieved within the same network of brain regions. Behaviorally, a spatial layout can be treated as a map[45] and therefore a coherent entity overall and, once well learned, can in principle be loaded and accessed quickly. We found that correct spatial retrieval was characterized by lower frequency interactions overall across the network along with early and prolonged increases in functional connectivity across the network compared to temporal order retrieval. In contrast, remembering temporal order

information involves traveling back in time to retrieve different temporal contexts[43,46,47], which would necessitate active comparison of each element within the sequence with the item to be compared. We found that temporal order retrieval was characterized by faster frequency interactions, a more delayed increase in network connectivity, and overall less coherence in time across the network compared to spatial retrieval. While somewhat speculative, these explanations provide possible insight into differences in how the brain is able to process aspects of space and time during memory retrieval. Specifically, our data lend support to the concept of spectrotemporal multiplexing[25, 27, 29] as a means to store and retrieve spatial and temporal context information encoded amongst neurons in the same regions. Our results thus provide a possible mechanism by which spatial and temporal contextual information, thought to underlie episodic memory[1,2], could be retrieved simultaneously. In our study, however, patients retrieved spatial and temporal context on separate trials, and it is not necessarily the case that the dynamics will be identical, for example, when spatial and temporal context are retrieved simultaneously, an issue future studies will need to address. Notably, a previous study during memory encoding[38] identified frequency–specific differences in spike–field coherence in the low–frequency band that predicted later retrieval, raising the possibility that spectrotemporal multiplexing is a general feature in episodic memory processes.

By employing direct intracranial recordings and a graph theoretic approach, our study provides a new perspective on how the human brain processes episodic memories. Our data provide novel support for models that emphasize global network interactions and frequency–specific connectivity, rather than regionally–mediated activity alone, as central to how we recover spatial and temporal memories associated with recent experiences. Our results thus argue for the importance of carefully timed dynamics across multiple brain regions as critical to spatiotemporal memory retrieval.

Online Methods

Patient electrophysiology

Six adult patients with medically refractory epilepsy underwent electrocorticography (ECoG) to localize seizures and participated in the study after providing informed consent approved by the University of Texas Medical Center committee for the protection of human subjects. Electrophysiological methods and electrode localization were similar to that described previously [48]. In brief, subdural circular platinum–iridium electrodes with a top hat design (4.5 mm overall diameter, 3 mm cortical contact, 10 mm interelectrode distance) were implanted and placed based solely on clinical considerations using standard techniques[49]. Electrode localization was verified by co–registering a post–operative CT image with a pre–operative MRI structural image. Lobar and gyral labels were assigned by an expert in human neuroanatomy (N.T.). Electrodes showing epileptiform activity based on neurologists evaluation were excluded from all analyses.

ECoG signals were sampled at 1000 Hz using Nihon Kohden NeuroFax software with a recording bandwidth from .15 to 300 Hz. Signals were referenced to a common average consisting of all non–ictal electrodes over lateral frontal and lateral temporal areas to

minimize the impact of the referencing scheme on synchronization measures[50]. Recordings were then imported into Matlab (MathWorks; Natick, MA) for post–processing.

Behavioral task

Patients played a virtual–taxi game similar to that used previously[24] with a few exceptions that were necessary to accommodate the clinical environment. The virtual environment consisted of 5 stores spaced irregularly and arranged in a circle (Figure 1D). Patients performed multiple blocks of navigation in which they picked up a passenger in the center of the environment and delivered them to a specific store (Figure 1C). This involved freely navigating the environment with a fixed order of visits to stores. Both the spatial layout of the environment and the delivery order were independent of each other[24] and maintained across blocks in order to subsequently test spatial layout and temporal order memory.

Following each block of navigation, patients performed interactive training emphasizing the spatial layout as a 2–D array and the temporal order of visits to stores as a 1–D sequence in time (Figure 1D). Interim testing was performed to emphasize the different characteristics of the spatial layout and temporal order of deliveries and to ensure that the patient had sufficient knowledge to accurately perform the final retrieval session. Interim testing involved the patient localizing each store onto a grid of the virtual environment viewed from an overview perspective or onto a timeline corresponding to the delivery order to stores (Figure 1D). The patient then viewed the correct answers displayed for 10 seconds separately for the spatial layout and the temporal sequence. The order of interactive training (spatial or temporal) was randomized following each block of navigation. Patients continued to perform multiple rounds of navigation and interactive training until they achieved either 100% accuracy on both spatial and temporal questions for two consecutive rounds or had completed eight rounds of navigation and interactive training.

During the final retrieval session (Figure 1E), which forms the basis of the results reported here, patients performed a block of spatial retrieval and a block of temporal retrieval trials, the order of which was counterbalanced across patients. The patient was provided with an image of the cue storefront along with two additional storefronts to choose from. The environment was arranged such that no two stores were ever the same distance apart. This generated 30 different possible unique trials for the spatial condition. During spatial retrieval trials, the patient was instructed to indicate which of the two stores was closer to the cue store in virtual space. For the temporal condition, we designed questions with the constraint that the choice stores either preceded or followed the reference store in time. This generated a total of 40 possible unique trials for the temporal condition. During temporal order retrieval trials, the patient indicated which of the two stores was closer to the cue store in delivery order. The number of trials analyzed for each patient in each condition is shown in Supplementary Table 2. One patient was excluded from the correct vs. incorrect analysis because they lacked sufficient incorrect responses. Responses for all portions of the paradigm described were subject paced to accommodate patient needs and the clinical testing environment; we therefore analyzed the fixed two second interval associated with cue onset during which subjects were instructed to begin retrieving from memory. We did this because we hypothesized that changes in activity related to retrieval would reliably

occur immediately after cue onset, consistent with previous studies[10]. The onset of the each trial was jittered uniformly from 1 to 1.5 seconds following subject response.

Phase synchronization estimation

All analyses used EEGLab[51] and custom–written code in Matlab. Raw EEG signals from the spatial and temporal retrieval session were extracted for both correct and incorrect responses from 1 second before to 2.2 seconds following cue onset in order to remove edge effects associated with spectrotemporal decomposition. Our primary behavioral contrasts were correct (spatial correct and temporal correct) vs. incorrect (spatial incorrect and temporal incorrect) and spatial correct vs. temporal correct. Phase synchronization estimates were computed between each pairwise combination of PHG (consisting of Parahippocampal, Perirhinal, and Entorhinal cortices), prefrontal (Superior & Middle Frontal Gyrus, Pars Triangularis), and parietal electrodes (Superior & Inferior Parietal Lobule, Precuneus) for each condition and contrast. Abbreviations for these regions are PHG, SFG, MFG, IFG, SPL, IPL, and PCN, respectively, and total pair counts are shown in Table S1. Phase estimates were obtained using a Hanning tapered fixed window length fast–Fourier transform (FFT) at 27 timepoints using the EEGLab "newcrossf" function from 2 to 1943 ms relative to cue onset and at 10 logarithmically spaced frequencies from .97 to 9.76 Hz. Frequencies were subsequently rounded to the nearest whole number. For analyses assessing phase synchronization to 200 Hz (Figure 4A and Supplementary Figure 7), we sampled a total of 40 logarithmically spaced frequencies such that each of the four frequency bins (1–10 Hz; 11–40Hz; 40–100 Hz; 100–200Hz) contained 10 sampled frequencies.

We estimated phase synchronization between electrode pairs at the above times and frequencies using the pairwise phase consistency (PPC) index in order to address issues associated with differing trial numbers between conditions[52]. Briefly, the PPC index for an electrode pair was estimated by first computing the relative phase angle difference between signals on each trial. The cosine was then computed between all pairwise (i.e., between trials) combinations of relative phases, and the PPC was taken as the mean of these cosine values. PPC values range from −1 to 1, with positive values indicating phase synchronization. We accounted for potential volume conduction confounds, which may artificially inflate phase synchronization estimates, by removing relative phases at 0 degrees (±5 degrees) prior to calculating the PPC index. We note that using standard phase coherence estimates or PPC estimates that included zero–phase synchronization did not qualitatively change our primary findings.

Network construction and statistical analysis

We utilized graph theoretic measures[34] to determine how functional interactions varied over time, frequency, and brain subregion. We considered a functional connection (i.e., edge) to exist between two subregions ("nodes") if there was a significant (bootstrap corrected $p<.05$, one–tailed paired t–test in order to test directionality) difference between conditions across all electrode pairs. Specifically, we compared PPC for one condition against a different condition across interregional electrode pairs, pooled across patients, and thus the degrees of freedom were the total number of electrode pairs in a comparison. To account for issues related to multiple comparisons and to maintain a fixed Type 1 error rate of 5 percent, we

estimated the distribution of t–values and shuffled the condition labels 1000 times before recomputing test statistics; observed t–values greater than the 95th percentile of this distribution were considered significant and were noted as significant connections (“edges”) in the network. This procedure was repeated separately at each time bin and at each frequency point (Figure 3). We then computed three basic measures of network connectivity. To assess the connectivity of a single node, we computed the total number of connections between a given node and all other connected nodes over time (0–2000 msec). We defined this to be node degree. To determine the relative strength of functional interactions between two nodes, (i.e. Figure 3C), we computed the total number of connections between those two nodes over time. Finally, we summed all connections in the network at a specific frequency over time, providing a frequency–specific measure of global functional interactions in the network. These measures were used for statistical testing (below), and were then converted to a percent connectivity measure. Percent connectivity was defined as the number of observed edges out of the total number of possible edges (accounting for the number of time, frequency, and interregional pairs sampled). Follow–up analyses using a more stringent bootstrap alpha of .001 (Supplementary Figure 10) were consistent with our primary findings.

In a random network, edges are uniformly distributed amongst nodes such that connectivity should not vary across regional pairs or frequencies[34]. Statistical analyses thus employed Chi Square tests to compare the distribution of edges and total number of connections for each node in the actual network against the null hypothesis that edges and number of connections were uniformly distributed.

To assess if edges were more clustered in time in the 2Hz Spatial or 8Hz Temporal networks, for each interregional pair, we extracted a binarized edge map, in which a 1 indicates a connected pair at a given time point and 0 indicates a lack of a connection. Binary vectors for each combination of interregional pairs (twenty interregional pairs chosen two at a time, n=190 pairs total) were then correlated using the Phi correlation coefficient, resulting in a distribution for each network. Differences between these distributions were assessed using a two–sample Kolmogorov–Smirnov test and additionally using paired t–tests. Follow–up analysis estimated the “chance” correlation by generating 1000 randomly seeded networks (matched for total number of edges in the 2Hz and 8Hz network using Monte Carlo simulations), re–calculating the mean Phi correlation across pairs, and extracting the 95th percentile of this distribution.

Statistical significance in our basic population analyses of task–related differences in PPC (i.e. Figures 2E,2F,5C; number of pairs for each comparison shown in Table S1) used family–wise error correction, with p_{fwe}=.05[53]. This corresponded to 4 contiguous time–frequency points each individually significant with a one–tailed paired t–test at $p < .005$. We note that the most significant time–frequency points held up to thresholding without cluster correction to at least p<.00001.

Supplementary Material

Refer to Web version on PubMed Central for supplementary material.

Acknowledgments

This work was supported by the Sloan Foundation, Hellman Young Investigator Award, and NINDS RO1NS076856. We thank Charan Ranganath and Andrew Yonelinas, as well as their lab members, along with 3 anonymous reviewers for helpful comments on this manuscript.

References

1. Eichenbaum H, Yonelinas AP, Ranganath C. The medial temporal lobe and recognition memory. Annu Rev Neurosci. 2007; 30:123–152. [PubMed: 17417939]
2. Mitchell KJ, Johnson MK. Source monitoring 15 years later: what have we learned from fMRI about the neural mechanisms of source memory? Psychol Bull. 2009; 135:638–677. [PubMed: 19586165]
3. Ranganath C, et al. Dissociable correlates of recollection and familiarity within the medial temporal lobes. Neuropsychologia. 2004; 42:2–13. [PubMed: 14615072]
4. Scoville WB, Milner B. Loss of recent memory after bilateral hippocampal lesions. J Neurol Neurosurg Psychiatry. 1957; 20:11–21. [PubMed: 13406589]
5. Squire LR, Stark CE, Clark RE. The medial temporal lobe. Annu Rev Neurosci. 2004; 27:279–306. [PubMed: 15217334]
6. Simons JS, Spiers HJ. Prefrontal and medial temporal lobe interactions in long-term memory. Nat Rev Neurosci. 2003; 4:637–648. [PubMed: 12894239]
7. Vargha-Khadem F, et al. Differential effects of early hippocampal pathology on episodic and semantic memory. Science. 1997; 277:376–380. [PubMed: 9219696]
8. Duarte A, Ranganath C, Knight RT. Effects of unilateral prefrontal lesions on familiarity, recollection, and source memory. J Neurosci. 2005; 25:8333–8337. [PubMed: 16148241]
9. Blumenfeld RS, Ranganath C. Prefrontal cortex and long-term memory encoding: an integrative review of findings from neuropsychology and neuroimaging. Neuroscientist. 2007; 13:280–291. [PubMed: 17519370]
10. Vilberg KL, Rugg MD. Memory retrieval and the parietal cortex: a review of evidence from a dual-process perspective. Neuropsychologia. 2008; 46:1787–1799. [PubMed: 18343462]
11. Spaniol J, et al. Event-related fMRI studies of episodic encoding and retrieval: meta-analyses using activation likelihood estimation. Neuropsychologia. 2009; 47:1765–1779. [PubMed: 19428409]
12. Hutchinson JB, Uncapher MR, Wagner AD. Posterior parietal cortex and episodic retrieval: convergent and divergent effects of attention and memory. Learn Mem. 2009; 16:343–356. [PubMed: 19470649]
13. Buzsaki G. The hippocampo-neocortical dialogue. Cereb Cortex. 1996; 6:81–92. [PubMed: 8670641]
14. Eichenbaum H. A cortical-hippocampal system for declarative memory. Nat Rev Neurosci. 2000; 1:41–50. [PubMed: 11252767]
15. Norman KA, O'Reilly RC. Modeling hippocampal and neocortical contributions to recognition memory: a complementary-learning-systems approach. Psychol Rev. 2003; 110:611–646. [PubMed: 14599236]
16. McClelland JL, McNaughton BL, O'Reilly RC. Why there are complementary learning systems in the hippocampus and neocortex: insights from the successes and failures of connectionist models of learning and memory. Psychol Rev. 1995; 102:419–457. [PubMed: 7624455]
17. Nadel L, Moscovitch M. Memory consolidation, retrograde amnesia and the hippocampal complex. Curr Opin Neurobiol. 1997; 7:217–227. [PubMed: 9142752]
18. Teyler TJ, DiScenna P. The hippocampal memory indexing theory. Behav Neurosci. 1986; 100:147–154. [PubMed: 3008780]
19. Fell J, Axmacher N. The role of phase synchronization in memory processes. Nat Rev Neurosci. 12:105–118. [PubMed: 21248789]
20. Benchenane K, et al. Coherent theta oscillations and reorganization of spike timing in the hippocampal-prefrontal network upon learning. Neuron. 66:921–936. [PubMed: 20620877]

21. Siapas AG, Lubenov EV, Wilson MA. Prefrontal phase locking to hippocampal theta oscillations. Neuron. 2005; 46:141–151. [PubMed: 15820700]
22. Sirota A, et al. Entrainment of neocortical neurons and gamma oscillations by the hippocampal theta rhythm. Neuron. 2008; 60:683–697. [PubMed: 19038224]
23. Spiers HJ, et al. Unilateral temporal lobectomy patients show lateralized topographical and episodic memory deficits in a virtual town. Brain. 2001; 124:2476–2489. [PubMed: 11701601]
24. Ekstrom AD, Copara MS, Isham EA, Wang WC, Yonelinas AP. Dissociable networks involved in spatial and temporal order source retrieval. Neuroimage. 56:1803–1813. [PubMed: 21334445]
25. Siegel M, Donner TH, Engel AK. Spectral fingerprints of large-scale neuronal interactions. Nat Rev Neurosci. 13:121–134. [PubMed: 22233726]
26. Donner TH, Siegel M. A framework for local cortical oscillation patterns. Trends Cogn Sci. 15:191–199. [PubMed: 21481630]
27. van der Meij R, Kahana M, Maris E. Phase-amplitude coupling in human electrocorticography is spatially distributed and phase diverse. J Neurosci. 32:111–123. [PubMed: 22219274]
28. Maris E, van Vugt M, Kahana M. Spatially distributed patterns of oscillatory coupling between high-frequency amplitudes and low-frequency phases in human iEEG. Neuroimage. 54:836–850. [PubMed: 20851192]
29. Canolty RT, et al. Oscillatory phase coupling coordinates anatomically dispersed functional cell assemblies. Proc Natl Acad Sci U S A. 107:17356–17361. [PubMed: 20855620]
30. Hipp JF, Hawellek DJ, Corbetta M, Siegel M, Engel AK. Large-scale cortical correlation structure of spontaneous oscillatory activity. Nat Neurosci.
31. Lega BC, Jacobs J, Kahana M. Human hippocampal theta oscillations and the formation of episodic memories. Hippocampus. 22:748–761. [PubMed: 21538660]
32. Anderson KL, Rajagovindan R, Ghacibeh GA, Meador KJ, Ding M. Theta oscillations mediate interaction between prefrontal cortex and medial temporal lobe in human memory. Cereb Cortex. 20:1604–1612. [PubMed: 19861635]
33. Lavenex P, Amaral DG. Hippocampal-neocortical interaction: a hierarchy of associativity. Hippocampus. 2000; 10:420–430. [PubMed: 10985281]
34. Bullmore E, Sporns O. Complex brain networks: graph theoretical analysis of structural and functional systems. Nat Rev Neurosci. 2009; 10:186–198. [PubMed: 19190637]
35. Watrous AJ, Fried I, Ekstrom AD. Behavioral correlates of human hippocampal delta and theta oscillations during navigation. J Neurophysiol. 105:1747–1755. [PubMed: 21289136]
36. Mormann F, et al. Independent delta/theta rhythms in the human hippocampus and entorhinal cortex. FrontHum Neurosci. 2008; 2:3.
37. Libby LA, Ekstrom AD, Ragland JD, Ranganath C. Differential connectivity of perirhinal and parahippocampal cortices within human hippocampal subregions revealed by high-resolution functional imaging. J Neurosci. 32:6550–6560. [PubMed: 22573677]
38. Rutishauser U, Ross IB, Mamelak AN, Schuman EM. Human memory strength is predicted by theta-frequency phase-locking of single neurons. Nature. 2010; 464:903–907. [PubMed: 20336071]
39. Rizzuto DS, et al. Reset of human neocortical oscillations during a working memory task. Proc Natl Acad Sci U S A. 2003; 100:7931–7936. [PubMed: 12792019]
40. Rizzuto DS, Madsen JR, Bromfield EB, Schulze-Bonhage A, Kahana MJ. Human neocortical oscillations exhibit theta phase differences between encoding and retrieval. Neuroimage. 2006; 31:1352–1358. [PubMed: 16542856]
41. Womelsdorf T, et al. Modulation of neuronal interactions through neuronal synchronization. Science. 2007; 316:1609–1612. [PubMed: 17569862]
42. Yonelinas AP, et al. Effects of extensive temporal lobe damage or mild hypoxia on recollection and familiarity. Nat Neurosci. 2002; 5:1236–1241. [PubMed: 12379865]
43. Zhang H, Ekstrom AD. Human Neural Systems Underlying Rigid and Flexible Forms of Allocentric Spatial Representation. Human Brain Mapping. (in press).

44. Marshuetz C, Reuter-Lorenz PA, Smith EE, Jonides J, Noll DC. Working memory for order and the parietal cortex: an event-related functional magnetic resonance imaging study. Neuroscience. 2006; 139:311–316. [PubMed: 16417974]
45. Tolman EC. Cognitive Maps in Rats and Men. Psychol Rev. 1948; 55:189–208. [PubMed: 18870876]
46. Howard MW, Kahana MJ. A distributed representation of temporal context. Journal of Mathematical Psychology. 2002; 46:269–299.
47. Tulving E. Episodic memory: from mind to brain. Annu Rev Psychol. 2002; 53:1–25. [PubMed: 11752477]
48. Conner CR, Ellmore TM, Pieters TA, DiSano MA, Tandon N. Variability of the relationship between electrophysiology and BOLD-fMRI across cortical regions in humans. J Neurosci. 31:12855–12865. [PubMed: 21900564]
49. Tandon, N. Textbook of epilepsy surgery. Informa Healthcare; New York, NY: 2008. Cortical mapping by electrical stimulation of subdural electrodes: language areas; p. 1001-1015.
50. Nunez, PL.; Srinivasan, R. Electric fields of the brain : the neurophysics of EEG. Oxford University Press, Oxford; New York: 2006.
51. Delorme A, Makeig S. EEGLAB: an open source toolbox for analysis of single-trial EEG dynamics including independent component analysis. J Neurosci Methods. 2004; 134:9–21. [PubMed: 15102499]
52. Vinck M, van Wingerden M, Womelsdorf T, Fries P, Pennartz CM. The pairwise phase consistency: a bias-free measure of rhythmic neuronal synchronization. Neuroimage. 51:112–122. [PubMed: 20114076]
53. Cox RW. AFNI: software for analysis and visualization of functional magnetic resonance neuroimages. Comput Biomed Res. 1996; 29:162–173. [PubMed: 8812068]

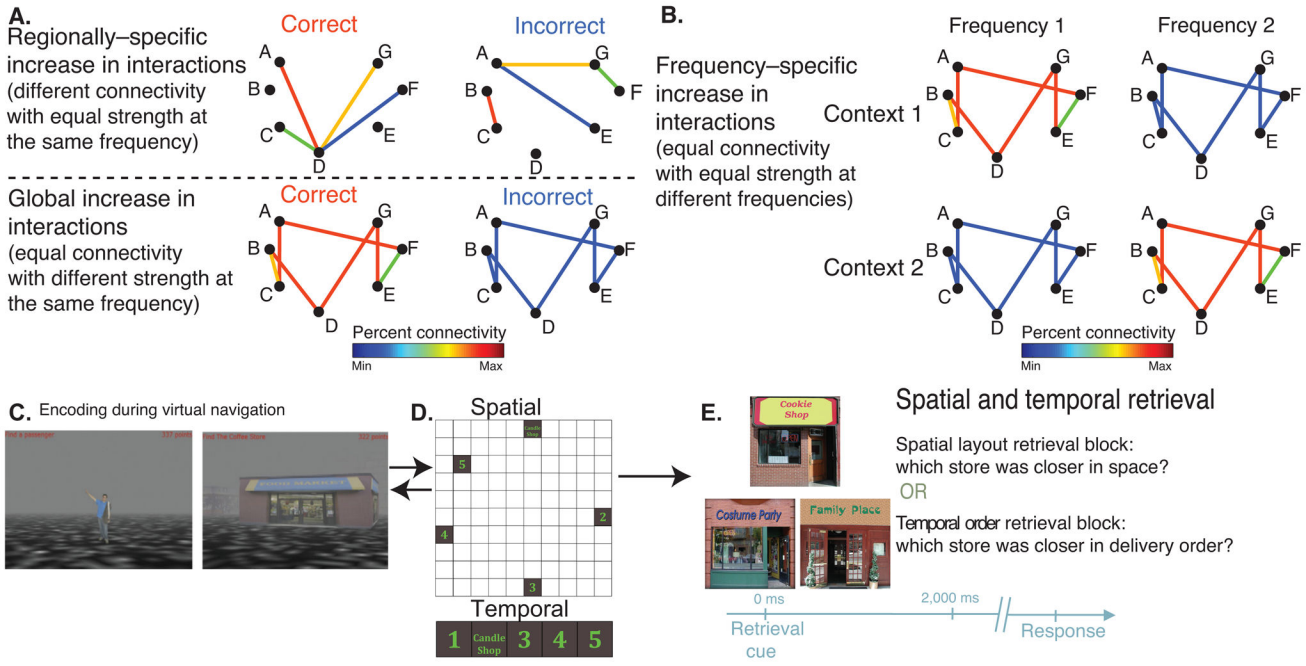

Figure 1. Different possible theoretical network architectures during memory retrieval

A) Memory retrieval may be accompanied by regionally specific network interactions (upper). Here, the same overall number and strength of connections are identical between networks, but the networks differ based on how regions (indicated by letters) interconnect. Alternatively, memory retrieval may be accompanied by a global increase in network interactions (lower). In this scenario, the same regions stay interconnected but the strength of network connectivity varies based on successful task performance. B) A third possibility is that the interregional connectivity pattern and strength are identical but the networks employ distinct phase–coupled frequencies to accomplish discrete processes. C–E) Experimental Set–up. Patients learned a spatial layout of salient landmarks and the temporal order of these same landmarks by performing a virtual navigation paradigm adapted from Ekstrom et al. 2011. Patients picked up passengers (C; left) in the center of the virtual environment and delivered them to specific locations (C; right). Following a round of navigation to all 5 stores, patient's interim spatial and temporal knowledge were tested using an interactive training task (examples shown in D). Patients performed multiple rounds of navigation and interactive training until they successfully learned the spatial layout and temporal delivery order (see Online Methods). E) Patients then performed a retrieval task and were presented with a cue store (e.g. "cookie shop") and two additional stores at time point zero. During the spatial retrieval block, patients were instructed to indicate which of the two stores shown was closer in space to the cue store; during the temporal retrieval block, patients were instructed to indicate which of the two stores was closer in delivery order to the cue store.

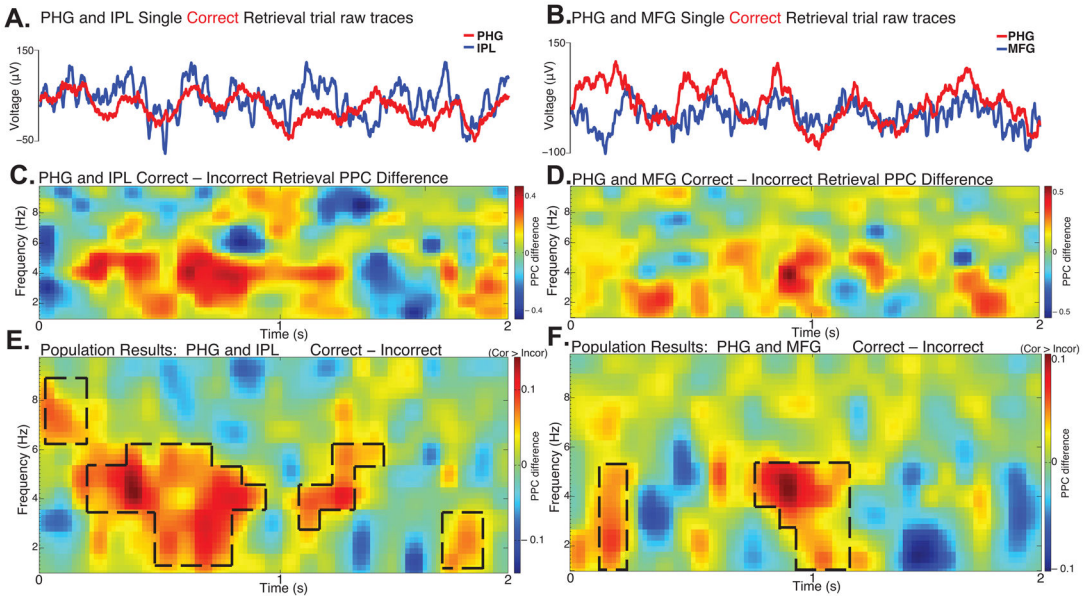

Figure 2. PHG–parietal and PHG–prefrontal phase synchronization during correct contextual retrieval

A,C,E) PHG & IPL phase synchronization during correct context retrieval. B,D,F) PHG & MFG phase synchronization during correct and incorrect retrieval. A) PHG & IPL raw ECoG traces from patient #3 during a single correct retrieval trial. The x–axis corresponds to that shown in (C). B) PHG & MFG raw ECoG traces recorded from patient #3 during a single correct retrieval trial. Electrode locations for traces shown in A and B are localized in Supplementary Figure 1 using green arrows. C) PPC difference map for correct vs. incorrect trials for the pair in A. Warmer colors indicate greater phase synchronization during correct retrieval. D) PPC difference map between correct and incorrect trials for the pair in B. E) Mean PPC difference between correct and incorrect retrieval across all PHG & IPL pairs (n=39). Dotted black boxes indicate significant differences between conditions ($p_{FWE}<.05$, see Methods). F) Mean PPC difference between correct and incorrect retrieval across all PHG & MFG pairs (n=125, significance testing identical to E). Additional raw trace examples for the pairs shown in A and B are shown in Supplementary Figure 2 & 3.

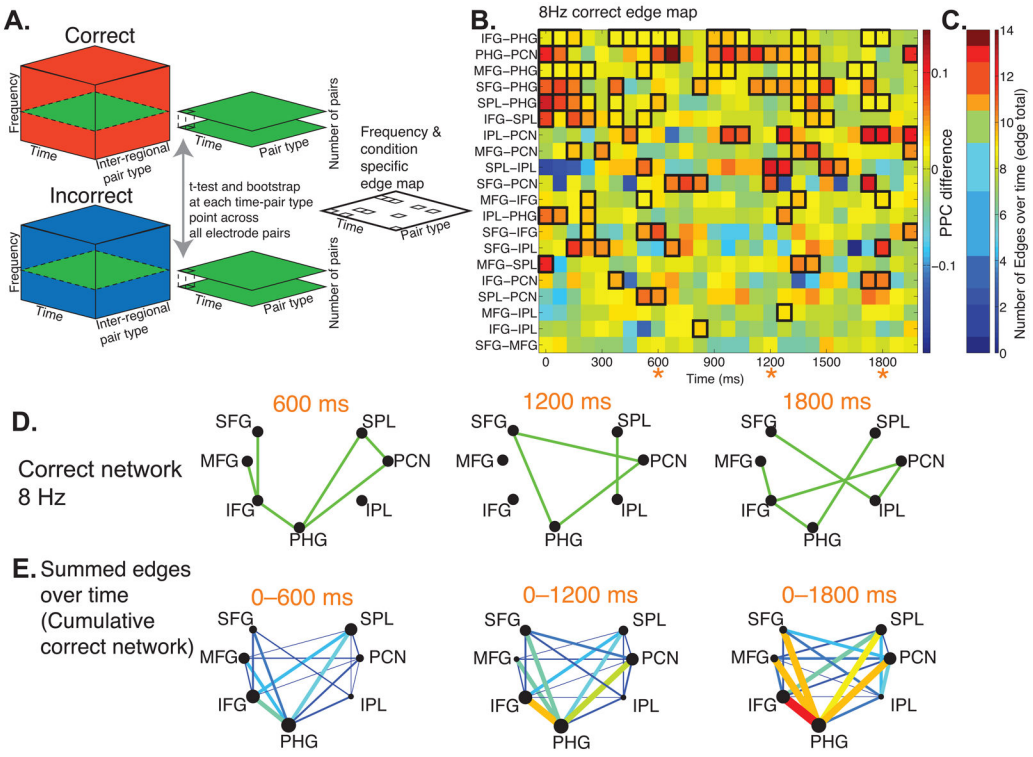

Figure 3. Memory–related network construction

Methods for characterizing frequency and condition specific memory networks. A) PPC values are pooled along the four dimensions of time, frequency, pair type (i.e. MFG & PHG, etc), and number of electrode pairs (not shown) for correct and incorrect trials. Comparing PPC during correct vs. incorrect retrieval and thresholding the resulting t–values (black boxes, $p<.05$, based on bootstrap resampling procedure) specify the time points at which specific interregional pairs show significant PPC differences for a given frequency and condition. B) Example connectivity map at 8Hz for correct retrieval, with black boxes showing significant edges, overlayed on the average correct minus incorrect PPC difference map. C) Colorbar showing the total number of significant differences between conditions in the 0–2000ms interval computed for each pair type. D) Network topology at three different time windows (orange asterisks in B) for the 8Hz correct retrieval networks. Green lines indicate a significant difference between conditions. E) Cumulative edges in three time windows for the 8Hz correct retrieval network. Color scale identical to (C).

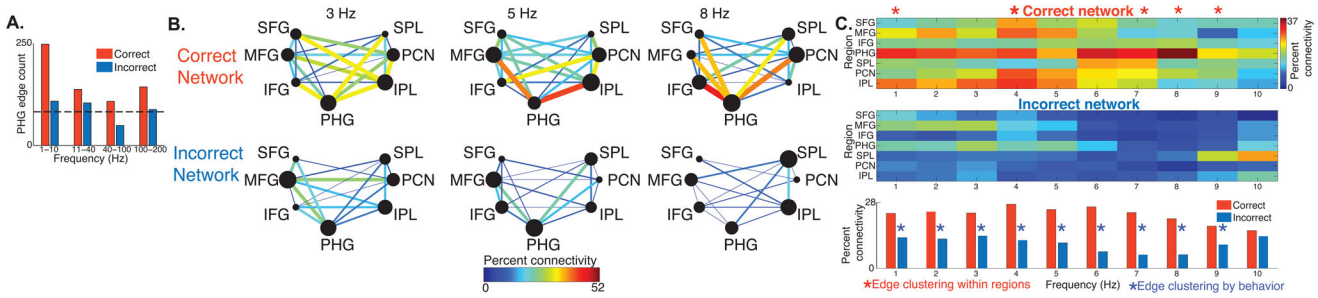

Figure 4.

Correct and incorrect memory networks. A) Total number of PHG connections in each condition as a function of 4 equal–sized frequency bins. The black dotted line indicates Type 1 error rate. B) Total number of connections, expressed as percent connectivity, between nodes for the correct vs. incorrect retrieval networks at 3, 5, and 8 Hz. Warmer colors indicate greater connectivity and the radius of each node shows the relative number of connections for that frequency and condition within a specific network; thus, node radius is not directly comparable between networks. C) Node degree, expressed as percent connectivity, in the correct (upper) and incorrect (middle) retrieval networks for each frequency. Total network connectivity for the correct and incorrect networks is shown below.

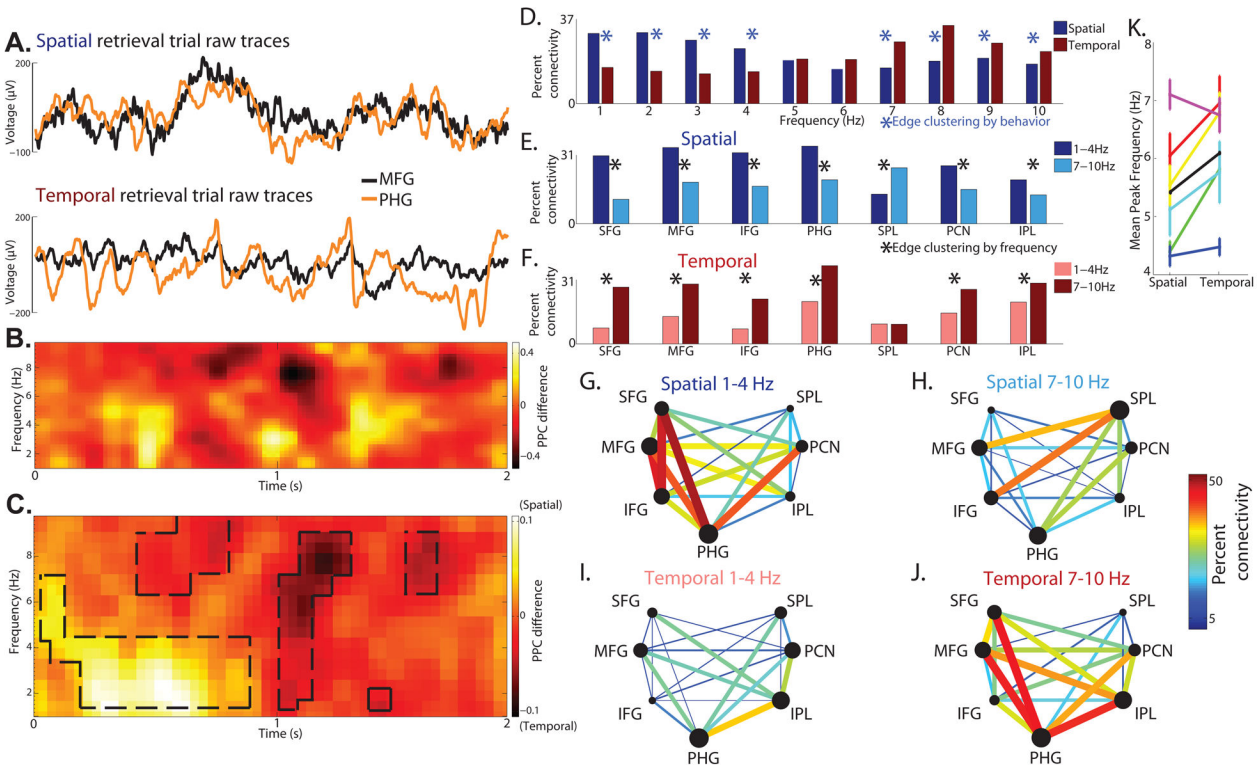

Figure 5. Frequency–specific synchronization during correct spatial and temporal context retrieval

A–C) MFG and PHG phase synchronization during correct spatial and temporal retrieval. A) Raw ECoG traces from patient #2 during a single spatial correct retrieval trial (upper) and a single temporal correct retrieval trial (lower). Electrode locations are shown in Supplementary Figure 1 as red arrows. B) PPC difference map between correct spatial and temporal trials for this pair. Lighter and darker colors indicate more phase synchronization during correct spatial retrieval and temporal retrieval, respectively. C) Mean PPC difference between spatial and temporal retrieval across all MFG and PHG pairs (n=189). Dotted black boxes indicate significant differences between conditions (p_{FWE}<.05), as in Figure 2E,F. D) Percent connectivity in the spatial and temporal retrieval networks as a function of frequency. E) Total number of connections, expressed as percent connectivity, in the spatial retrieval network shown for 1–4Hz and 7–10Hz frequency bands. F) Similar to (E), except for the temporal retrieval network. G–J) Correct spatial and temporal retrieval networks in the 1–4 Hz and 7–10 Hz bands. K) Average peak frequency for the spatial and temporal networks averaged across all PHG–frontal and PHG–parietal pairs represented separately for each patient using different colors. The black line shows the mean across subjects. Error bars indicate the standard error of the mean across pairs.

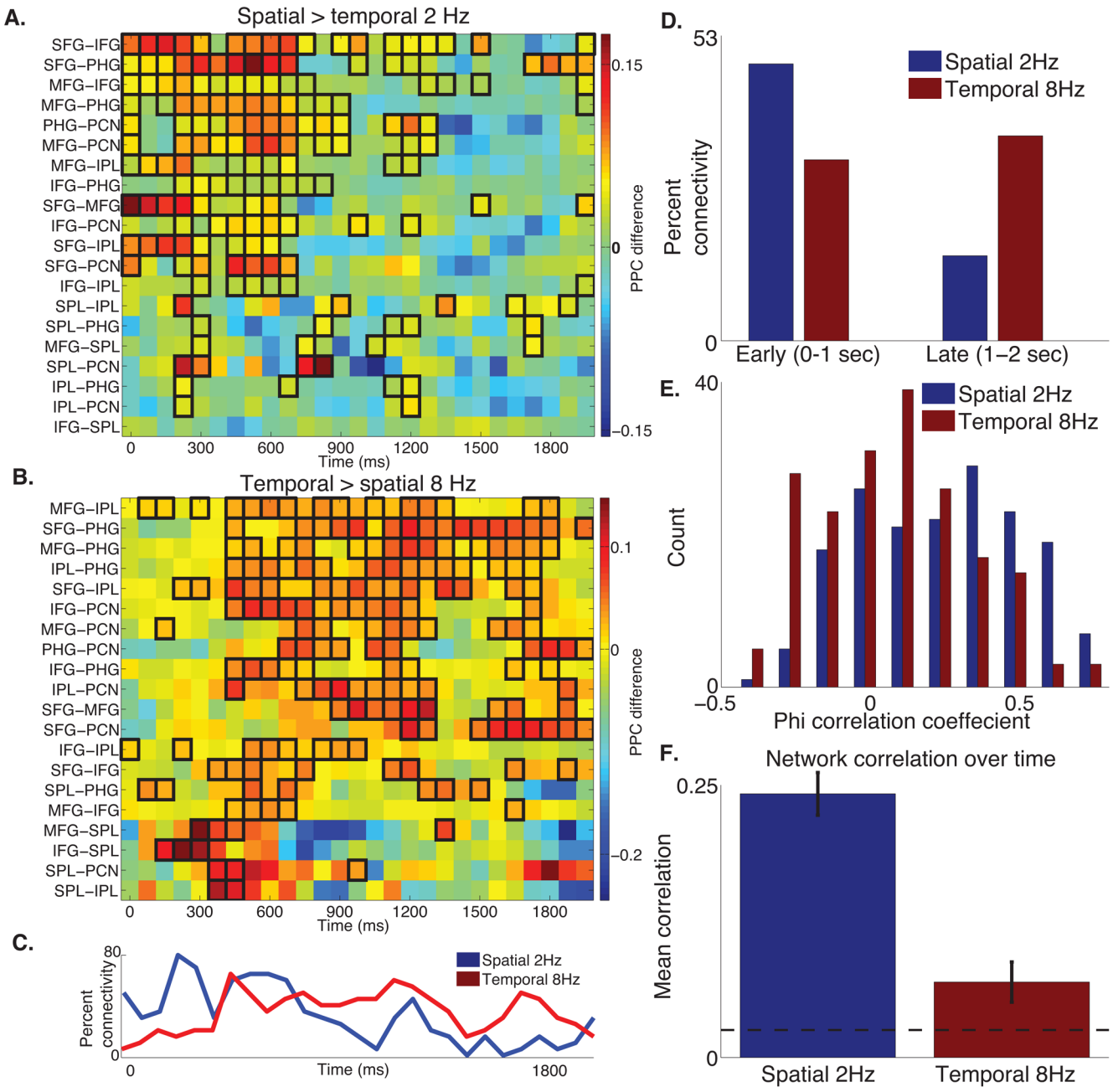

Figure 6. Differential patterns of connectivity over time during spatial and temporal context retrieval

A) Spatial > temporal PPC difference at 2 Hz for all interregional pairs across time. Significant differences are assessed between conditions across the population of all pairs in a region (black boxes indicate edges, bootstrap $p<.05$) at each time point (similar to Figure 3B). B) Similar to A), except showing temporal > spatial PPC difference at 8 Hz for all interregional pairs across time. C) Percent of total connections (out of 20 pairs) over time derived from 6A and 6B. D) Percent connectivity in these networks during 0–1 seconds and 1–2 seconds following cue onset. E) Distribution of correlation coefficients for the 2Hz and

8Hz networks (see Methods). F) Mean correlation coefficient for the 2Hz and 8Hz networks. Dotted black line indicates bootstrap–estimated 95th percentile derived from randomly generated networks (see Methods). Similar results were observed in adjacent frequencies (Supplementary Figure 9A). Error bars denote standard error of the mean across interregional pair combinations (n=190).